A Systematic investigation on structural and optical properties of sol-Gel spin coating fabricate CdS Nanocrystalline thin films: Effect of Ni doping

BRIJLATA SHARMA (briji1985@gmail.com)
BIT DURG: Bhilai Institute of Technology https://orcid.org/0000-0003-4121-5510
Rajesh Lalwani
BIT DURG: Bhilai Institute of Technology
Ruby Das
BIT DURG: Bhilai Institute of Technology
Devi Singh Raghuwanshi
Shri Shankaracharya Technical Campus

Research Article

Keywords: Nanocrystalline CdS, Thin films, XRD, Optical bandgap, Photoluminescence

Posted Date: March 17th, 2021

DOI: https://doi.org/10.21203/rs.3.rs-309135/v1

Version of Record: A version of this preprint was published at Journal of Materials Science: Materials in Electronics on July 20th, 2021. See the published version at https://doi.org/10.1007/s10854-021-06606-x.

A Systematic investigation on structural and optical properties of sol-Gel spin coating fabricate CdS Nanocrystalline thin films: Effect of Ni doping.

Brijlata Sharma[1]*, Rajesh Lalwani[1] , Ruby Das[1] and Devi Singh Raghuwanshi[2]

[1]*Department of Applied Physics, Bhilai Institute of Technology, Durg(C.G.)-491001, India*
[2]Department of Physics, Shankaracharya Technical Campus, Bhilai (C.G.) India 490020.

***(Corresponding author: Email:** briji1985@gmail.com**)**

Abstract

In the present work, we have successfully fabricated undoped and Ni-doped Nanocrystalline CdS thin film on an ultrasonically cleaned glass substrate employing the Sol-Gel spin coating technique. The structural and spectroscopic properties of the films were investigated using XRD spectra, UV-Vis spectroscopy and photoluminescence spectra respectively. The X-Ray diffraction spectra revealed the polycrystalline nature of films with cubic structure and (111) as preferred orientation. The average particle size evaluated by the Debye-Scherrer formula lying in the range 6.65nm to 12.05 nm for the deposited films. According to UV-VIS Spectroscopy, the average transmittance of films in the visible region varies between 70% to 90%. The optical band gap of CdS thin film was evaluated from absorption spectra. The bandgap of the deposited films is in the range of 2.48 eV to 2.70 eV which is higher than that of bulk CdS (2.42eV). This verifies the blue shifting in band edge of CdS Nanocrystalline thin films due to the quantum confinement effect. Photoluminescence spectra of the thin film showed that the fundamental band edge emission peak centred at 485nm also called blue band emission.

Keywords: Nanocrystalline CdS, Thin films, XRD, Optical bandgap, Photoluminescence.

Introduction

CdS thin film belong to one of the most important II-IV semiconductors with a direct bandgap of 2.42eV at room temperature [1,2]. II-IV semiconductors have special optoelectronic properties and potential application [3]. Large range applications of CdS Nanocrystalline materials have been studied such as photoconductors [4], photodetectors [5], and energy storage devices due to their high stability, good physical, chemical and optical properties which are different from bulk CdS. The application of CdS nanocrystalline thin films in energy conversion devices such as solar cell is the field of interest for many researchers [6-8]. The structural and optical properties of CdS can be tailored by doping it

with transition metal ions such as Fe, Co, Ni, Cu etc. [9,15]. Transition metal doped semiconductors are known as dilute magnetic semiconductor. Doping material is contained in the crystalline lattice during the deposition process which results in a significant change in the semiconductor material without changing its crystal structure. The bandgap of the material changes in comparison to its bulk materials and also there is a change in the luminescent property of the materials as the doped ions act as the recombination centres for the charge carriers in the conduction band [16-18].

There are various reports on synthesis and characterisation of Ni-doped CdS nanocrystals by different deposition methods such as successive ionic layer adsorption and reaction (SILAR) [19], chemical vapour deposition (CVD) [20], thermal evaporation [21], atomic layer deposition (ALD) [22], spray pyrolysis [23], RF sputtering [24], molecular beam epitaxy (MBE) [25]. But, most of these techniques can be used for fabricating small area thin films; moreover, they are extortionate and time taking process. Large scale fabrication of CdS nanostructures especially controlled synthesis of high-quality nanostructured CdS thin films through a solution based route at low temperatures still remains a challenging job for material scientists. The Spin coating method [26-28] is one of the simplest, cost-effective, eco-friendly and large area thin film deposition technique. The spin coating technique has many advantages such as minimal matter wastage, economical way of large-area fabrication, and no manoeuvre of toxic gases. In the present work, we use a simple and low-cost spin coating technique for the deposition of Ni-doped CdS Nanocrystalline thin films. The change in optical, structural and surface properties have been studied to find the utilization of CdS thin films in optoelectronic devices.

1. **Experimental Arrangement**:

The well adherent, uniform high-quality Undoped and Ni-doped Nanocrystalline CdS films were fabricated by Spin Coating Method. For the deposition of films, $CdCl_2$ and thiourea were used as the source of Cd^{2+} and S^{2-} ions. All the chemicals used were AR grade from Sigma Aldrich. Firstly solutions were prepared by dissolving 0.3M of $CdCl_2$ and 0.3M thiourea in 2-Methoxyethonal separately and kept for constant stirring for 30 minutes. After this, the solutions were mixed and 2.5ml of Monoethanolamine was added and the obtained solution was again stirred vigorously for 30 minutes and then the solution was rested for 1.5 hr. Now the different amount of Ni doping was added in the prepared solution of CdS. The different compositions of the solution were named as, sample Ni_00 (undoped CdS), sample

Ni_01 (1ml Ni), sample Ni_02 (2ml Ni), Sample Ni_03 (3ml Ni), Sample Ni_04 (4ml Ni), Sample Ni_05 (5ml Ni). Before depositing the films, the glass substrates were dipped in HNO_3(Nitric acid) for 24 hrs and then cleaned using detergent and washed in the ultrasonic cleaner by triple distilled water and dried in air. The fresh solution was used for the deposition of thin films. The solution was dropped in glass substrate which was then kept in spin coater at 3600 RPM for 45 s. After deposition, the samples were kept in a Furnace at 150oC for 15 minutes to evaporate the solution. This procedure of deposition and drying was repeated 7 times. The Optical absorption and transmission spectra for all deposited films were recorded over the wavelength range 400–800 nm using UV–Vis spectrophotometer CHEMITO SPECTRASCAN-2600. The photoluminescence spectra of the deposited films were recorded using a constant deviation spectrometer over the visible range 400–700 nm. UV source with filters from 235 to 320 nm was used as an excitation source. A photomultiplier tube (RCA931A), was used to detect emitted light and finally, the emitted light output was recorded in the form of current using a digital Pico-ammeter(DPM-121, SES, Roorkee, India). The X-ray diffraction patterns for the structural properties of prepared films were examined by using D8 Advance X-ray diffractometer with CuKairradiation (l= 1.54060 Å) and operated at 40 kV and 100 mA.

1. **Results and Discussion**

3.1 XRD Studies

X-ray diffraction technique was used for the structural analysis of undoped and Ni-doped nanocrystalline CdS thin films. Fig.1 shows the X-ray diffraction plot of the samples of undoped and Ni-doped nanorystalline CdS thin films. All the observed peaks fit well with polycrystalline face centred cubic CdS crystal structure (JCPDS Card No. 80-0019). The broaden peaks in the XRD patterns indicate the nanocrystalline behaviour of the particles. The XRD spectra illustrate the peak corresponding to (111) and (220) lattice planes of zinc blend structure. Also as observed from the spectra the peak that depicts the (111) plane acquire maximum intensity, followed (220) with the approximately same amplitude. Moreover, the intensity and width of the peak increase slightly with an increase in Ni doping concentration. The peak intensity certainly stimulated on increasing doping concentration; in such a way that it becomes more intense, revealing enhancement of crystallinity of CdS thin films. Moreover, no impurity peaks were noticeable in diffractograms within the sensitivity of XRD. As the radius of Ni (0.83 Å) is smaller than that of Cd (1.08 Å), the substitution of

Ni in CdS lattice will decrease the lattice constant. Therefore, in XRD spectra a slight shift of diffraction peak towards a higher angle is observed. The Interplanner Spacing was calculated by Bragg's Equation[29].

$$2dsin\theta = n\lambda \qquad \text{.....(1)}$$

where, is interplanar spacing, is Bragg's angle, is the order of spectrum, is the wavelength of x-ray used. The lattice constant has been evaluated using equation[30]

$$d_{hkl} = \frac{a}{\sqrt{(h^2+k^2+l^2}} \qquad \text{.....(2)}$$

where hkl is the miller indices. The calculated interplanar spacing and lattice constant values are shown in Table 1. The volume of a unit cell is also calculated by

The variation of peak position (2θ), FWHM, d-spacing values, lattice parameters, and volume of cell are listed in table 1.The crystallite size of nanocrystalline thin films was evaluated from the full width at half maximum (FWHM) from the strongest peak (111) plane using Scherrer's equation [31]and is tabulated in Table 1.

$$D = \frac{0.9\lambda}{\beta cos\theta} \qquad \text{..... (3)}$$

where is the crystallite size, is FWHM (Full width half maxima), is the wavelength of x-ray used. The crystallite size of the Nanocrystalline CdS films slightly decreased with an increase in Ni doping concentration. The values of the crystallite size of the films were found to be in the range 12.05 – 6.65 Å. The growth direction of the Nanocrystalline thin films remains unaffected by the amount of doping, but it helps the grain growth down to an optimal concentration of doping. The decrease of nanocrystallite size results in increasing the defects in the deposited thin films.

The dislocation density(δ) was calculated using the Williamson and Smallmans formula[32]

$$\delta = \frac{1}{D^2} \text{…..... (4)}$$

The dislocation density of undoped nanocrystalline CdS thin film was found to be6.88 x 1017 nil/m2, and it increases with increasing Ni doping. The strain which is associated with "misfit" in lattice depends on the growth condition of the films. The Strain (ε) was evaluated using relation[33]

$\varepsilon = \frac{\beta cot\theta}{4}$ .....(5)

It is noticed that the value of strain of Ni-doped Nanocrystalline CdS films shows a slight increase with increasing Ni concentration. With an increase in Ni doping concentration, the strain value increases and the grain boundaries decrease significantly because of the smaller particle size. The values of crystallite size, dislocation density and strain are calculated and listed in table2.

3.2 Optical Properties

The optical studies like absorption, transmission, refractive index and bandgap energy are adored in optoelectronic applications. The UV-VIS spectrophotometer was used to study the optical behaviour and energy gap of materials. The optical absorbance and transmittance spectra of undoped and Ni-doped nanocrystalline CdS thin films deposited on a glass substrate at room temperature are shown in Fig.2. The absorption and transmission curve of undoped and Ni-doped CdS Nanocrystalline thin films were taken in the wavelength range 400-900nm. All films have a uniform pattern of absorption. They show lower absorption in the higher wavelength region while in the lower wavelength region it increases sharply. There is an increase in absorbance of films with increasing Ni concentration. The films having maximum Ni concentration has the highest absorption while the undoped film has the lowest absorption. All the films exhibit high transmittance, throughout the UV-VIS-NIR region. The usual behaviour of absorption and transmission spectra is the increase of transmittance with wavelength while at lower wavelength region the transmittance was nearly zero. The film with a low Ni doping concentration shows higher transmittance in the visible range. This may be owing to the good crystallinity of the films; this result is in good agreement with XRD results.

After comparison of absorbance and transmittance of undoped and Ni-doped CdS Nanocrystalline thin films. The optical bandgap was evaluated by the Tauc method; the optical absorbance region defined according to the following equation [37]

$(\alpha hv)^{\frac{1}{n}} = A(hv - E)$ .....(6)

where A is a proportionality constant, Eg is bandgap and n is constant which designate the type of transition. The type of transition is estimated by a plot of

(αhυ)2 versus hυ which is a linear graph as shown in Fig.3. As the graph is linear, the transition is a direct transition and its value is taken as ½ for an allowed direct transition. The bandgap Eg can be evaluated by extrapolating the linear portion of the graph. The bandgap of undoped and Ni-doped Nanocrystalline CdS thin films are in the range 2.48 – 2.70 eV and is tabulated in the table.2, which is comparatively higher than bandgap of bulk CdS (2.42eV). The bandgap value is increasing gradually with an increase in doping concentration and this arises the phenomenon of blue shift in transmittance spectra and the increased value of bandgap can be assigned to quantum confinement effect. The refractive index of deposited films gives knowledge such as film density, cavities in the film, speed of light in the films etc. It was evaluated by the Herve-Vandamme formula[33]

$$\mathbf{n^2 = 1 + (\frac{A}{Eg+B})^2} \text{.....(7)}$$

where A & B are constants having value 13.6 eV and 3.4 eV. The refractive index found to decrease from 2.51 to 2.43 for all the deposited films. Refractive index changes also account for crystallite size and internal strain of the film. The decreasing value of the refractive index conveys a reduction in the crystallite size of films.

The extinction coefficient computes the amount of light loss owing to scattering and absorption per unit volume of penetrating medium. The extinction coefficient (k) was evaluated by using equation[34]

$$\boldsymbol{k = \frac{\lambda \alpha}{4\pi}} \text{.....(8)}$$

Where α is the absorption coefficient and λ is the wavelength.

Fig. 3 shows the extinction coefficient versus wavelength for undoped and Ni-doped CdS Nanocrystalline thin films. It has the highest value for undoped CdS thin films at a lower wavelength and its value decreases with increasing doping concentration. The extinction coefficient decreases gradually with an increase in wavelength. This verifies that with increasing wavelength there is a decrease in loss of light by scattering as well as by absorbance.

The crystallite size was computed by effective mass approximation formula [33]

$$E_g = E_g(bulk) + \frac{2\hbar^2\pi^2}{\mu D^2} \quad \text{.....(9)}$$

Where D is the diameter of crystallite and μ is the effective mass of electron-hole pair. The

the computed value of crystallite size is tabulated in table 3.

3.3 Photoluminescence Analysis:

Photoluminescence is a technique in which electrons are excited by a monochromatic light source that undergoes radiative recombination either at valence band or surface states. PL study is used to investigate the optical characteristic of semiconductors thoroughly. PL spectra of undoped and Ni-doped CdS nanocrystalline thin films at an excitation wavelength of 400 nm are shown in Fig.4. A single peak was observed for pure and doped samples corresponding to radiative recombination of free excitons or the band to band transition. Sharp PL peak was observed at 480nm for undoped and Ni-doped CdS Nanocrystalline thin film which is due to blue emission. The blue emission is due to the direct band transition of CdS. PL spectra of deposited films clearly show that with increased Ni concentration the intensity of PL peaks also increases. The increase in intensity can be attributed to the change in the crystal structure and crystalline size. All the films show a shifting of peak in the lower wavelength region. The film having 5ml Ni doping shows a decrease in intensity and a peak shift towards the lower wavelength region. On comparing the PL emission of bulk CdS (512nm) with Ni-doped CdS Nanocrystalline thin films. The position of band to band PL transition reveals a blue shift which assigns a strong quantum confinement effect.

Electrical properties

Electrical Resistivity of undoped and Ni-doped Nanocrystalline CdS thin films were measured using two-point DC probe method under dark media. The measurement was taken in the range of 323-473K. Fig shows a graph of log (resistivity) versus inverse absolute temperature.

On increasing the temperature, the resistivity of deposited films decreases which verify the semiconducting nature of films. The resistivity of undoped and Ni-doped Nanocrystalline CdS thin films are in the range 10^7-10^3 Ωcm. There is a decrease in the resistivity of films due to doping. Resistivity decreases almost 10^4 times on doping. The undoped CdS films have the highest resistivity this might be by the virtue of the defects and dislocations present in the film. The resistivity of films decreases by doping Ni this might be because of enhancement in the structural properties and film crystallinity which is in good agreement with the XRD results.

The conductivity of deposited films is calculated by using equation

$$\boldsymbol{\sigma = Ae^{\frac{-Ea}{kbT}}} \text{.....(10)}$$

Where A is the pre-exponential factor, E_a is the Activation energy, kb is Boltzmann's constant and T is the absolute temperature. The conductivity of undoped and Ni-doped Nanocrystalline CdS thin films are in the range of 10^{-7}-10^{-3} mhocm^{-1}. There is an increase in the conductivity of films due to doping.

According to Arrhenius plot E_a is the slope of a plot of log(conductivity) against 1/T. The slope of the above plot can be determined as follows

Equation (3) can be written as

$\ln(\sigma) = \ln(A)$ slope $(\frac{1}{T})$ .....(**11**)

The value of slope can be determined from a linear plot of log(conductivity) against 1/T.

$$slope = \frac{\log(\sigma 2) - \log(\sigma 1)}{\frac{1}{T2} - \frac{1}{T1}} \text{.....(12)}$$

The Activation energy (Ea) is calculated as

$$Ea = -Kb\ X\ Slope \text{.....(13)}$$

as the slope is negative, the value of activation energy will be positive.

The calculated activation energy of undoped CdS Nanocrystalline thin film was found to be 0.5604 eV and for Ni-doped films it was found in the range 0.4595 -0.1851 eV. Thus the film with maximum doping concentration has the highest conductivity and lowest activation

energy. Thus increased conductivity for film maximum doping concentration reveals that it is appropriate for numerous electronic applications.

1. Conclusion

The structural and optical properties of nanocrystalline CdS thin films were investigated with Ni doping. The undoped and Ni-doped CdS nanocrystalline thin films were successfully deposited on a suitably clean glass substrate using the Sol-gel spin coating method. All samples in the present study were found to be oriented along the (111) direction with a small reflection from (220) and have a cubic type structure. No secondary phases for Ni were observed. The XRD studies also reveal that the deposited films have a crystalline size in the range of 12.05 nm to 6.65 nm. The optical studies show that undoped and Ni-doped films have high transmittance in the range of 70-90% and found that Ni doping increases the bandgap up to 2.70 eV. Ni doping shifts the absorption edge significantly towards the lower wavelength region. For Ni-doped nanocrystalline CdS thin films, the optical band gap energy range is between 2.48 eV and 2.70 eV. Bandgap energy of the nanocrystalline thin films is greater than that of the bulk CdS thin films, which is a confirmation of the quantum confinement effect. Photoluminescence studies show that the undoped nanocrystalline CdS thin films have an emission peak in the blue region at 485nm at it shifts toward the lower wavelength region with increasing Ni doping. The electrical study reveals that the resistivity of films decreases and conductivity of films increases with increasing doping concentration. The activation energy of films decreases with increasing Ni doping concentration. Thus all the above properties reveals that it is appropriate for numerous electronic and optoeletronic applications.

Acknowledgements

We are thankful to TEQIP III, CSVTU Bhilai, India for providing financial assistance under the Collaborative Research Scheme (CRS). We are also grateful to the management of Bhilai Institute of Technology, Durg, for providing lab facilities. We also acknowledge UGC-DAE consortium for Scientific Research, Indore, India for providing XRD Measurements at their consortium.

References

1. K.C. Wilson, E. Manikandan, M. Basheer Ahamed, B.W. Mwakikunga, Nanocauliflower like structure of CdS thin film for solar cell photovoltaic applications: In situ tin doping by chemical bath deposition technique. Journal of Alloys and Compounds **585**, 555–560 (2014)
2. M. Afzaal, P. O'Brien,Recent development in II-VI and III-VI semiconductor and their applications in solar cell. J. Mater. Chem. **16**, 1597 (2006)
3. N. Badera, B. Godbole , S.B. Srivastava, P.N. Vishwakarma , L.S. Sharath Chandra, Deepti Jain, Mohan Gangrade, T. Shripathi , V.G. Sathe , V. Ganesan Quenching of photoconductivity in Fe doped CdS thin films prepared by spray pyrolysis technique. Applied Surface Science **254**, 7042-7048 (2008)
4. T. Gao, Q.H. Li,T.H. Wang, CdS nanobelts as photoconductors. Appl. Phys. Lett.**86**, 173105 (2005)
5. N. Kouklin, L. Menon, A. Z. Wong, D. W. Thompson, J. A. Woollam, P. F. Williams,S.Bandyopadhyay, Giant photoresistivity and optically controlled switching in self –assembled nanowires. Appl. Phys. Lett. **79** ,4423 – 4425 (2001)
6. W. Lee, S.H. Kang, S.K. Min, Y.E. Sung, S.H. Han, Co-sensitization of vertically aligned TiO2 nanotubes with two different sizes of CdSe quantum dots for broad spectrum. Electrochem. Commun. 10, 1579(2008)
7. W. Lee, W.C. Kwak, S.K. Min, J.C. Lee, W.S. Chae, Y.M. Sung, S.H. Han, Spectral broadening in quatum dots-senitized photochemical solar cells based on CdSe and Mg-doped CdSe nanocrystals. Electrochem.Commun. **10**, 1699 (2008)
8. W. Lee, J. Lee, S. Lee, W. Yi, S.H. Han, B.W. Cho, Enhanced charge collection and reduced recombination of CdS/TiO2CdS/TiO2 quantum-dots sensitized solar cells in the presence of single-walled carbon nanotubes. Appl. Phys. Lett. **92**, 153510 (2008)
9. N. Badera, B. Godbole , S.B. Srivastava, P.N. Vishwakarma , L.S. Sharath Chandra, Deepti Jain, Mohan Gangrade, T. Shripathi , V.G. Sathe , V. Ganesan Quenching of photoconductivity in Fe doped CdS thin films prepared by spray pyrolysis technique. Applied Surface Science **254**, 7042-7048 (2008)
10. A. Sarem, B.J. Kowalski, B.A. Orlowski, Optical properties of Fe-based semimagnetic semiconductors. J. Phys. Condens. Matter **2** ,8173 (1990)

11. Z.K. Heiba, M.M. Bakr, N.G. Imamc, Biphasic quantum dots of cubic and hexagonal Mn-doped CdS; necessity of Rietveld analysis. J. Alloys Compd. **618**, 280–286 (2015)
12. K.S. Rathore, D. Deepika , N.S. Patidar, K.B. Saxena ,Effect of Cu doping on the structural,optical and electrical properties of CdS nancrystales. J. Ovnic.Res 5,175 (2009)
13. S.Kumar, N Kumari, S.Kumar ,S. Jain, N. K. Verma,Synthesis and characterization of Ni-doped CdSe nanoparticles:magnetic studies in 300–100 K temperature range. Appl Nanosci **2**,437–443 (2012)
14. D. Acosta, C. Magana, A. Martinez, A. Maldonado, Structural evolution and optical characterization of indium doped cadmium sulphide thin filmsobtained by spray pyrolysis for different substrate temperatures. Sol. Energy Mater.Sol. Cells **82,** 11-20 (2004)
15. A.Fernandez-perez, C.Navarrete, P.Valenzuela, W.Gacitúa,E.Mosquera, H.Fernández, Characterization of chemically- deposited aluminium doped CdS thin films with post-deposition thermal annealing. Thin Solid Films **623**, 127-134 (2017)
16. S. Rai, L. Bokatial, Effect of CdS nanopartiles on photoluminescence spectra of Tb^{3+} in sol-gel- derived silics glasses. Bull.Mater. Sci.**34**, 227 (2011)
17. M.Thambidurai, N. Muthukumarasamy, D. Velauthapillai,C.Lee, Quantum confinement effects in Gd-doped CdS nanopartiles prepare by chemical precipitation technique. Mater,J.Sci.mater.Electron. **24,**4535-4541 (2013)
18. K.S.Kumar, A. Divya, P.S. Reddy, Synthesis and characterization of Cr doped CdS nanoparticles stabilized with polyvinylpyrrolidone. Appl. Surf. Sci. **257**, 9515-9518 (2011)
19. K.C. Preetha, K.V.Murali, A.J.Ragina, K.Deepa, T.L.Remadevi, Effect of cationic precursor pH on optical and transport properties of SILAR deposited nano crystalline PbS thin films. Current Applied Physics,vol.**12(1)**, 53-59 (2012)
20. D.Barreca, A.Gasparotto, C.Maragno, E.Tondello, CVD of Nanosized ZnS and CdS thin films from single-source precursors. J. Elecrochem.Soc. **151(6)**,pp.G4 28-35 (2004)
21. T.Gao, T.H.Wang, Catalyst-Assisted Vapor-Liquid-Solid Growth of Single-Crystal CdS Nanobelts and Their Luminescence Properties" J. Phys. Chem. B, vol. **108(52)**, pp. 20045-20049 (2004)

22. W.Lee, N.P. Dasgupta, J.H. Jung, J.Lee, R.Sinclair, B.F.Prinz, ScanningTunneling Spectroscopy of Lead Sulfide Quantum Wells Fabricated by Atomic Layer Deposition**.** *Nanotechnology*, vol. **21**, pp. 485402 (2010)

23. S.Pence, E.Varner, W.Clayton, Jr.Bates, Substrate temperature effects on the electrical properties of CdS films prepared by chemical spray pyrolysis. Mater. Lett., vol. **23**, pp. 13- 16x (2010)
24. I.Plaza, G. Diaz-González, F.Sánchez-Quesada, M. Rodríguez-Vidal, Structural and optical properties of r.f.- sputtered CdS thin films. Thin Solid Films, vol. **120**, pp. 31-6x(2010)
25. S.Petillona, A. Dinger, M. Grün, M.Hetterich, V.Kazukauskas, C. Klingshirn, Molecular beam epitaxy of CdS/ZnSe heterostructures," J. Cryst. Growth, vol. **201-202**, pp. 453-56 (1999)
26. Munirah, M.S. Khan A.Aziz , S.A.Rahman , Z.R.Khan , Spectroscopic studies of sol–gel grown CdS nanocrystalline thin films for optoelectronic devices. Materials Science in Semiconductor Processing **16** ,1894–1898 (2013)
27. I.Rathinamala, J.Pandiarajan, N.Jeyakumaran ,N.Prithivikumaran,Synthesis and Physical Properties of nanocrystalline CdS Thin Films – Influence of sol Aging Time & annealing Temperature. Int. J. Thin Film Sci. Tec. 3, No. 3, 113-120(2014)
28. T. Chtouki ,Y. El Kouari ,B. Kulyk , A. Louardi , A. Rmili , H. Erguig , B. Elidrissi ,Soumahoro , B. Sahraoui , Spin-coated nickel doped cadmium sulfide thin films for third harmonic generation applications. Journal of Alloys and Compounds 696, 1292-1297 (2017)
29. R. Das, R. Kumar, Preparation of nanocrystalline PbS thin films and effect of Sn doping and annealing on their structural and optical properties. Mater. Res. Bull. **47** 239-246 (2012).
30. R.Das, R. Kumar, Structural, photoluminescence and optical properties of chemically deposited $(Cd_{1-x}Bi_x)S$ thin films as a function of dopant concentration. J Mater Sci: Mater Electron **24** 697-703 (2013).
31. P.K. Sahu, R.Das, R. Lalwani, Preparation of nanocrystalline Mg doped CdSe thin films and their optical, photoluminescence, electrical and structural characterization. J Mater Sci: Mater Electron **28** 18296- 18306 (2017)
32. A.Oudhia, N. Shukla, P.Bose, R.Lalwani, A. Choudhary, Effect of various synthesis protocols on doping profile of ZnO:Eu Nanowires. Nano-Structures & Nano-Objects **7** 69-74 (2016)

33. P.K. Sahu, R.Das, R. Lalwani, Incorporation of tin in nanocrystalline CdSe thin films: a detailed study of optoelectronic and microstructural properties. App. Phy. A 124665 (2018)
34. R. Lalwani ,R. Das, Preperation and determination of optical constants of Nanocrystalline PbS thin films. ISSN:2348-604X(p)(2015)
35. R. Das, R. Kumar, Effect of annealing and composition on crystal structure, surface morphology and optical absorption of chemically deposited $Cd_{1-x}Sn_xS$ films. Cryst. Res. Technol. **45(7)** 725-731 (2010).

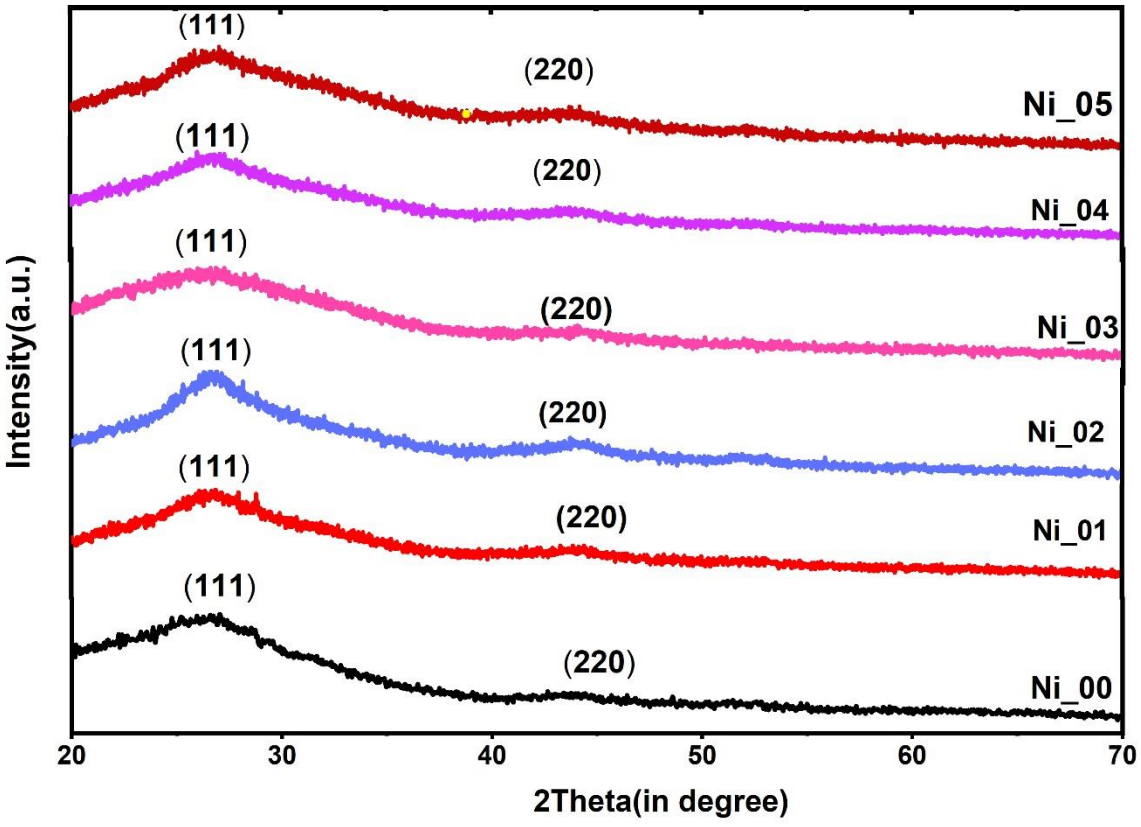

Fig.1. X-ray diffraction patterns for the undoped and Ni doped nanocrystalline CdS thin films.

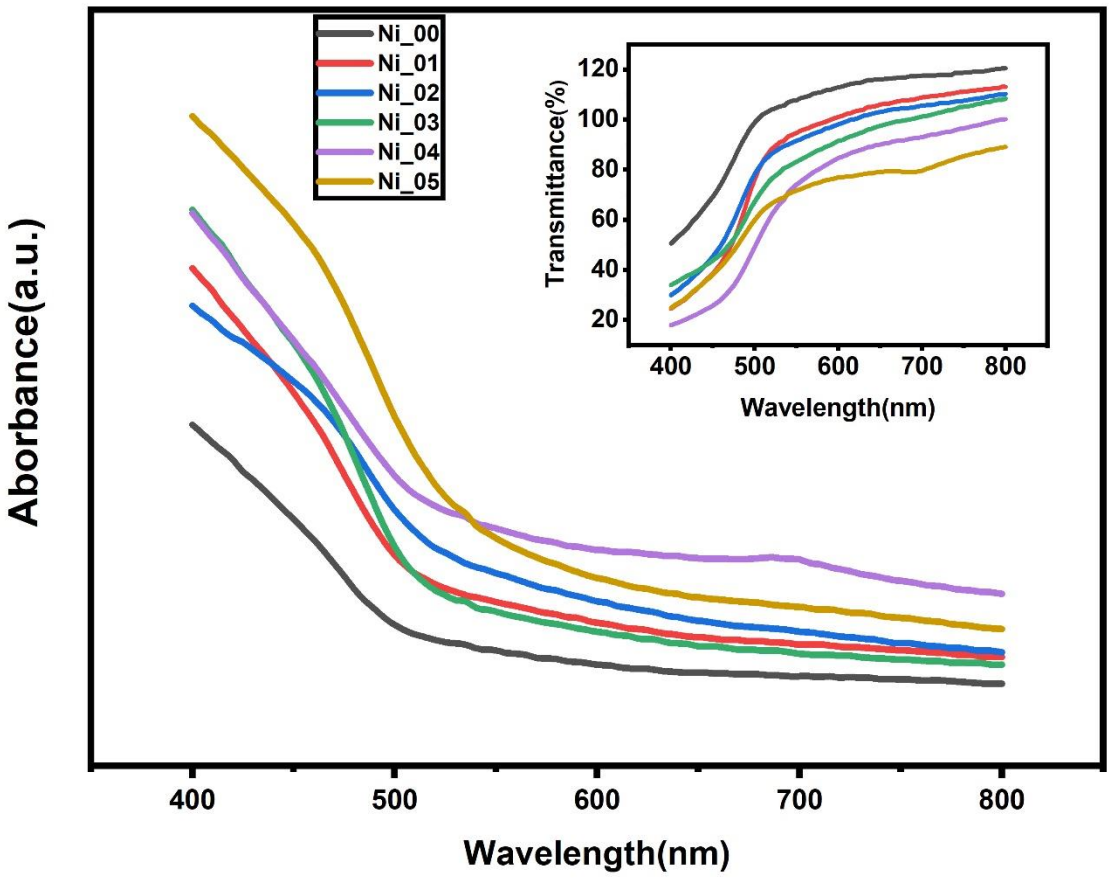

Fig.2. Optical Absorption and Transmission Spectra of undoped and Ni doped nanocrystalline CdS thin films.

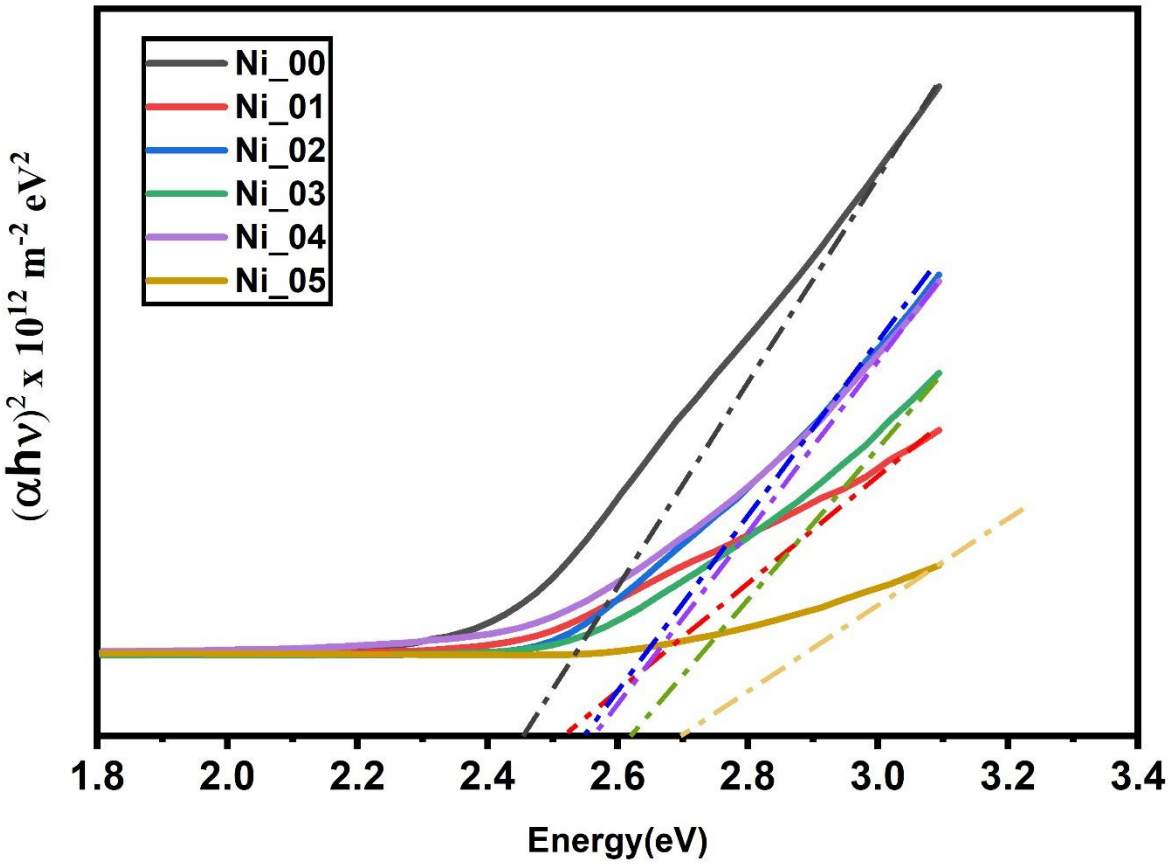

Fig.3. The Tauc's plot of nanocrystalline CdS thin films of undoped and Ni doped nanocrystalline CdS thin films.

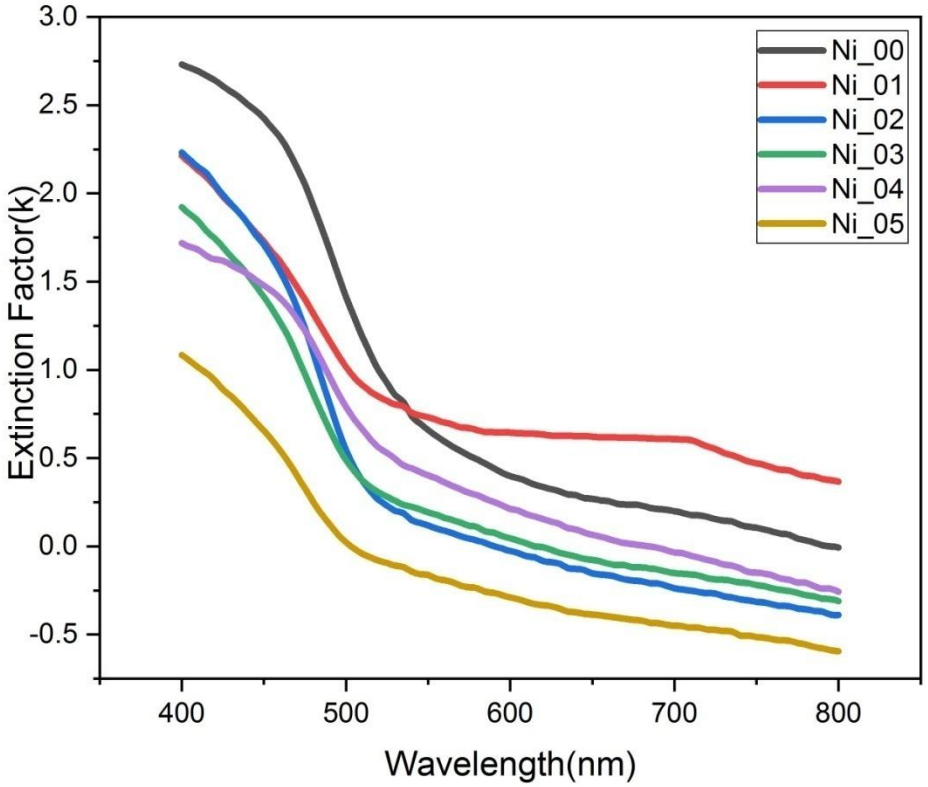

Fig.4. The Extinction Coefficient plot of nanocrystalline CdS thin films of undoped and Ni doped nanocrystalline CdS thin films.

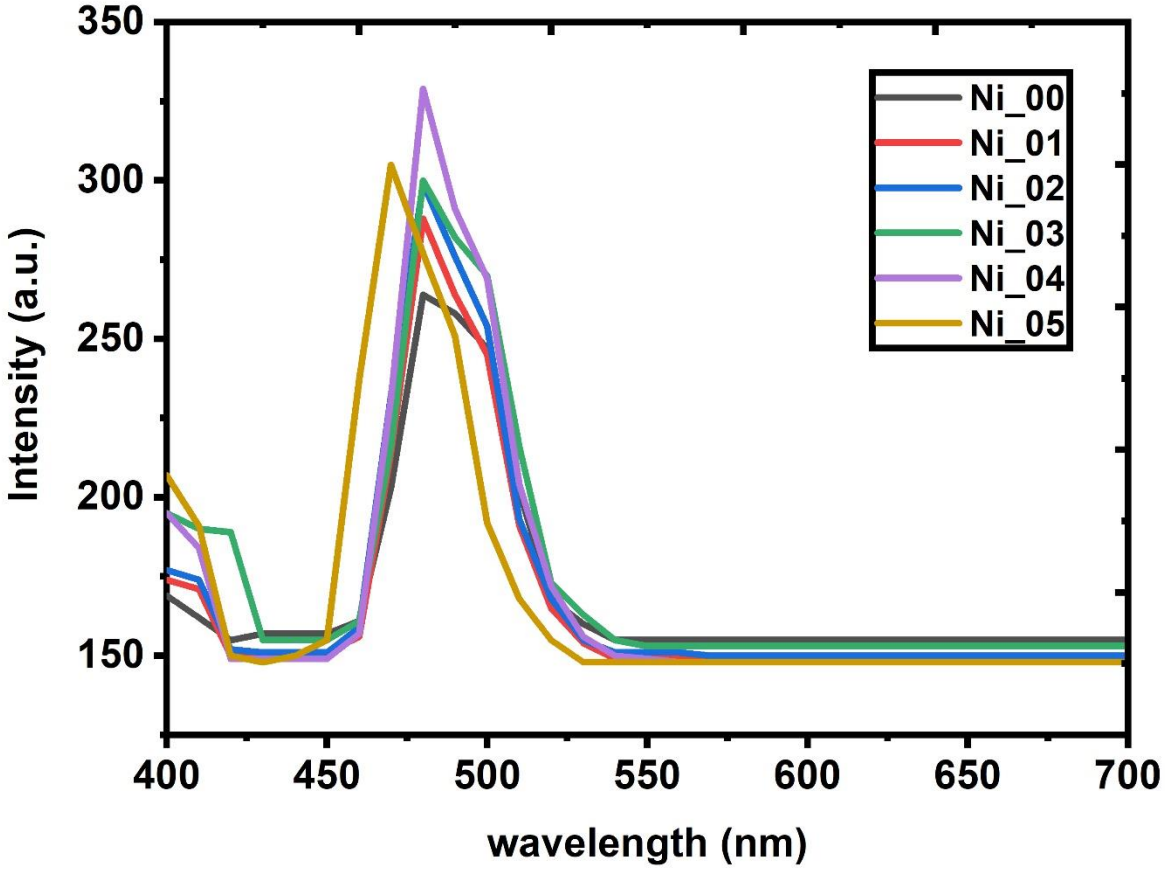

Fig.5. Photoluminescence spectra of nanocrystalline CdS thin films of undoped and Ni doped nanocrystalline CdS thin films.

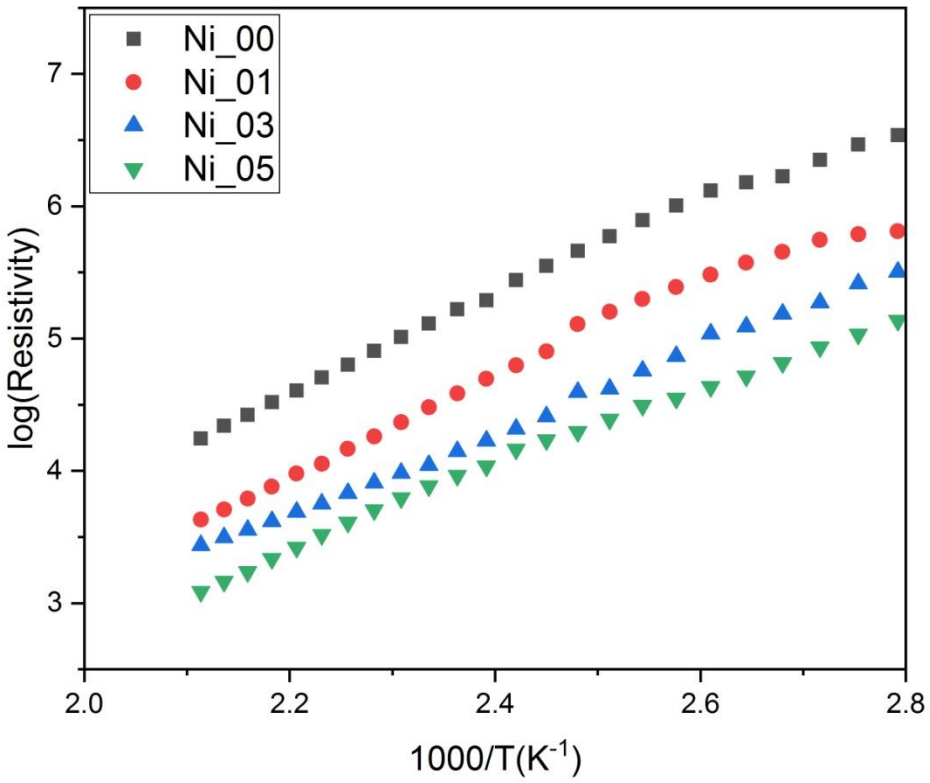

Fig-6 The plot of resistivity versus Temperature of nanocrystalline CdS thin films of undoped and Ni doped nanocrystalline CdS thin films

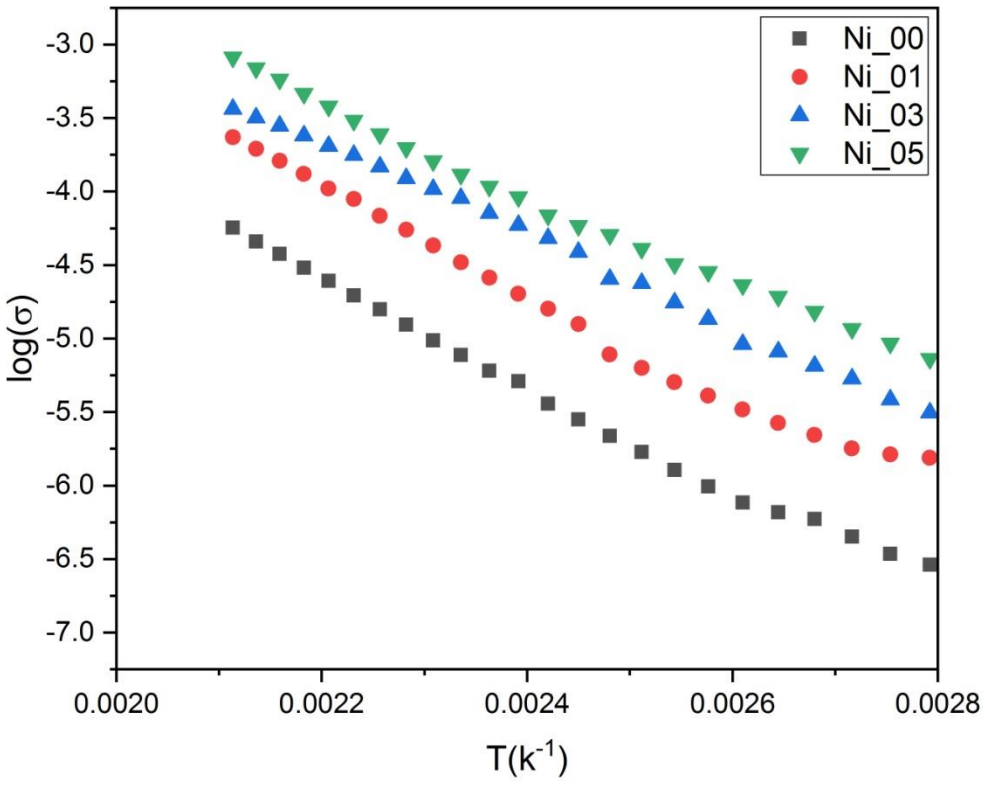

Fig-7 The plot of conductivity versus Temperature of nanocrystalline CdS thin films of undoped and Ni doped nanocrystalline CdS thin films

Table 1 Values of 2θ and hkl, d-spacing Lattice constant (a), volume of unit cell of Ni doped nanocrystalline CdS thin films.

Samples	**2θ**	**hkl**	**FWHM (β) (Theta)**	***d*-spacing (Å)**	**Lattice Constant (a) Å**	**Volume of unit cell**
Ni_00	26.28	(111)	6.61	3.39	5.87	198.86
Ni_01	26.4	(111)	8.64	3.37	5.84	179.42
Ni_02	26.44	(111)	8.82	3.37	5.83	185.94
Ni_03	26.97	(111)	9.56	3.30	5.72	202.45
Ni_04	27.05	(111)	11.45	3.29	5.70	187.57
Ni_05	27.38	(111)	11.98	3.25	5.64	199.75

Table 2 Values of Crystallite size (D), Strain (ε), Dislocation density (δ) of undoped and Ni doped nanocrystalline CdS thin films

Samples	**Crystallite Size (D) (nm)**	**Strain (ε) ($lin^{-2}m^{-4}$)**	**Dislocation Density (δ) ($x10^{17}lin/m^2$)**
Ni_00	12.05	0.122	6.88
Ni_01	9.24	0.154	11.70
Ni_02	9.04	0.160	12.22
Ni_03	8.33	0.178	14.39
Ni_04	6.96	0.208	20.59
Ni_05	6.65	0.222	22.59

Table 3 Values of band gap and refractive index of undoped and Ni doped nanocrystalline CdS thin films

Sample No.	**Bandgap(eV)**	**Shift in Bandgap(in eV)**	**Refractive Index**	**D(nm)**
Ni_00	2.48	0.06	2.51	12.76
Ni _01	2.52	0.10	2.50	9.89
Ni _02	2.54	0.12	2.48	9.67
Ni _03	2.56	0.14	2.46	8.36
Ni _04	2.62	0.20	2.45	7.00
Ni _05	2.70	0.28	2.43	5.97

Figures

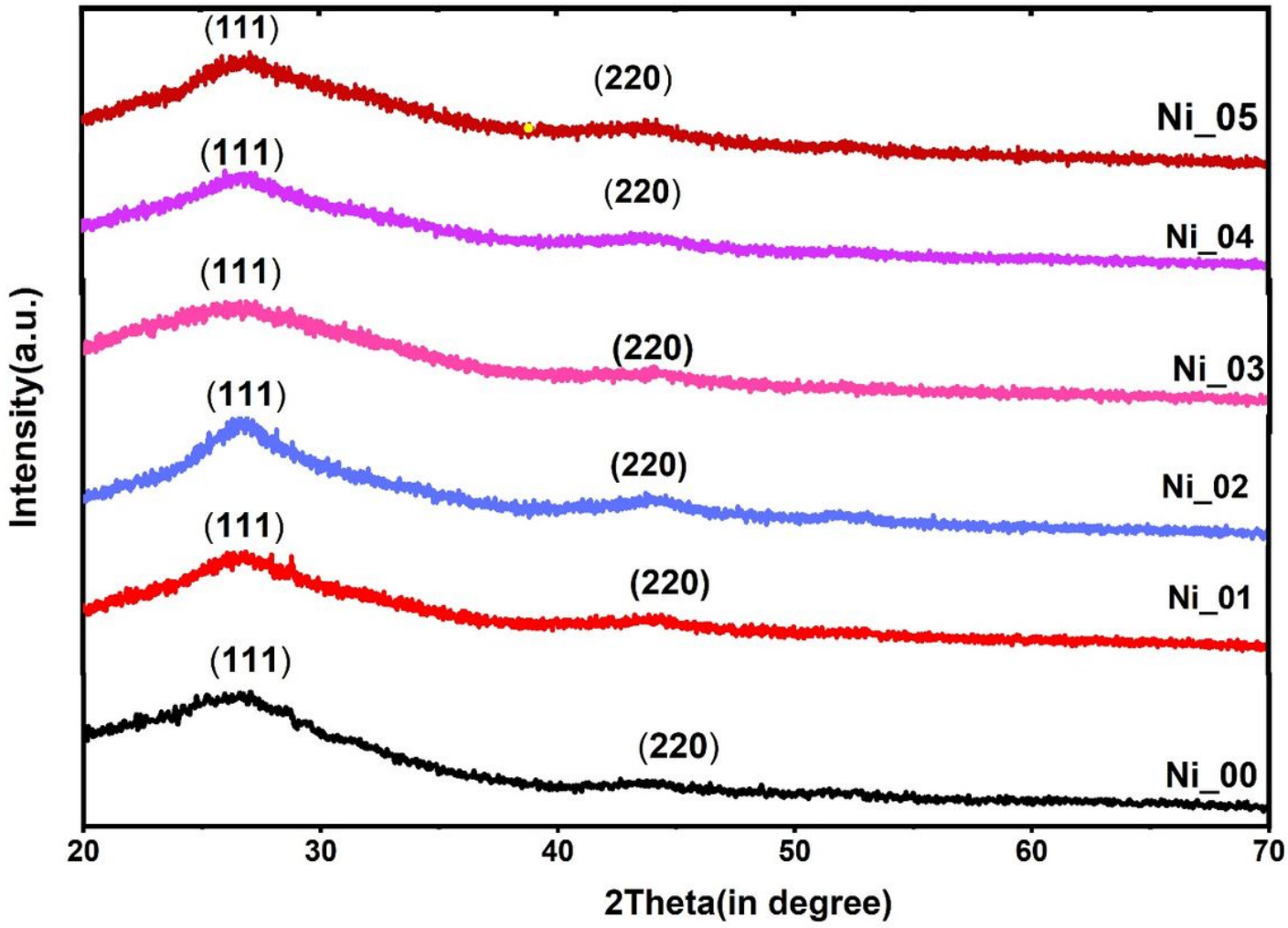

Figure 1

X-ray diffraction patterns for the undoped and Ni doped nanocrystalline CdS thin films.

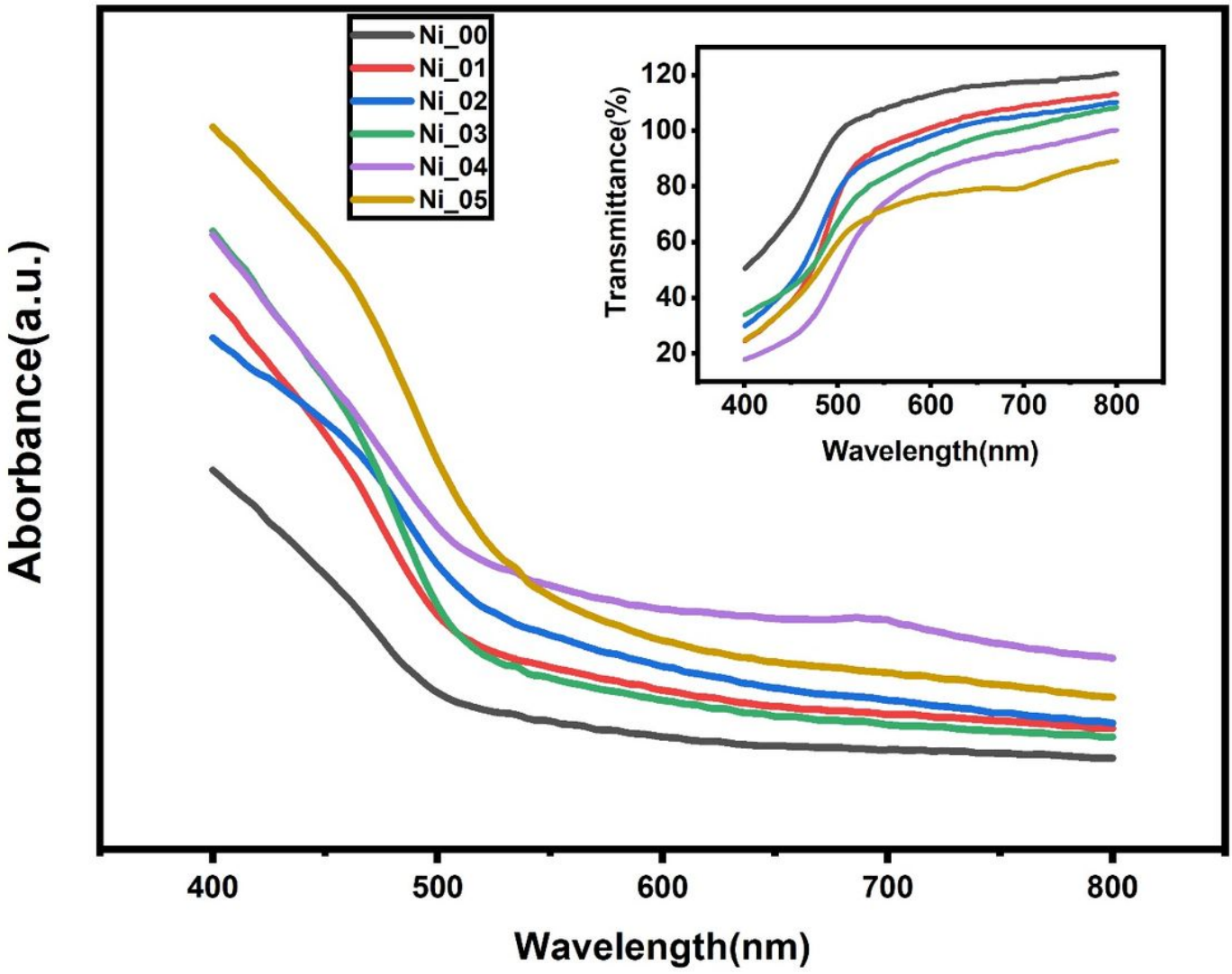

Figure 2

Optical Absorption and Transmission Spectra of undoped and Ni doped nanocrystalline CdS thin films.

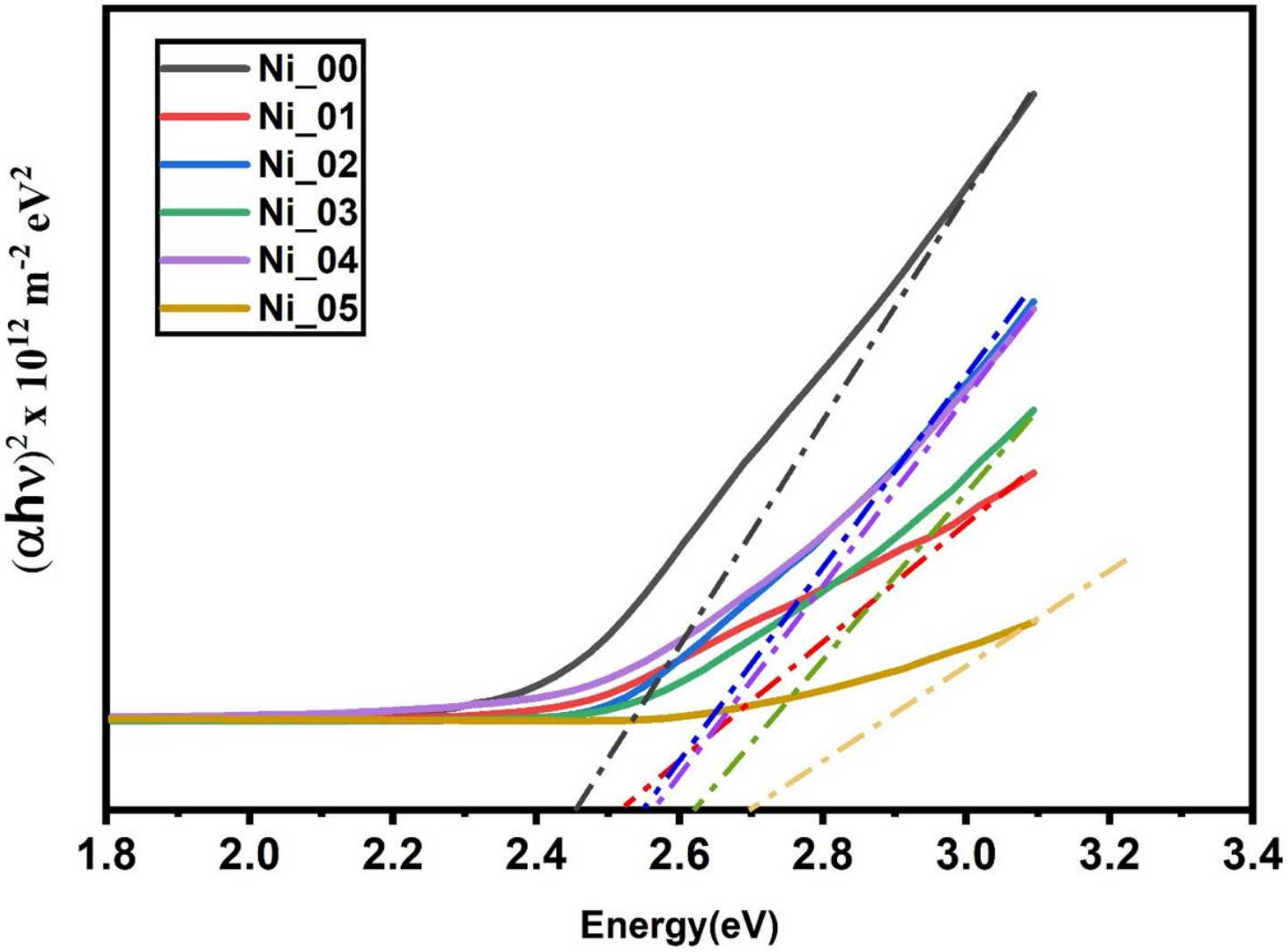

Figure 3

The Tauc's plot of nanocrystalline CdS thin films of undoped and Ni doped nanocrystalline CdS thin films.

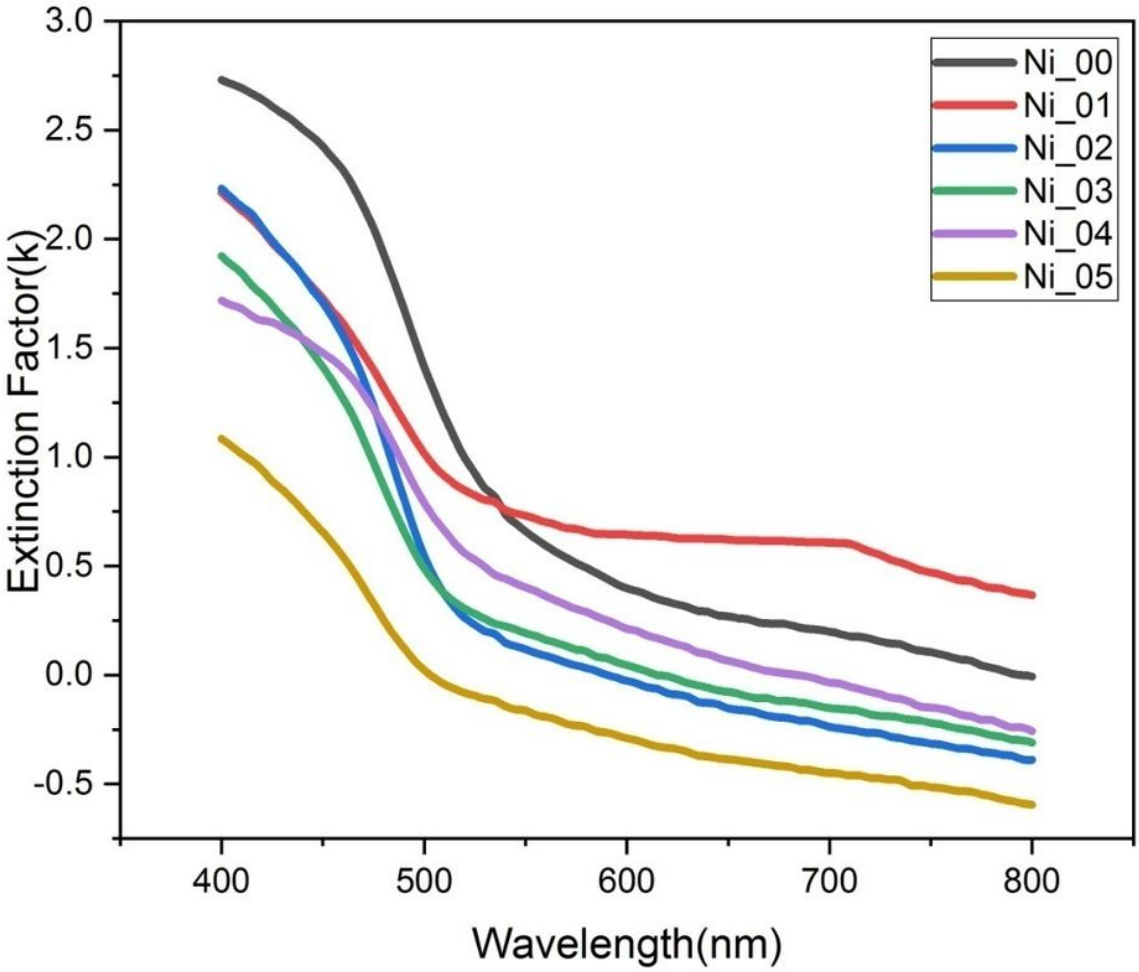

Figure 4

The Extinction Coefficient plot of nanocrystalline CdS thin films of undoped and Ni doped nanocrystalline CdS thin films.

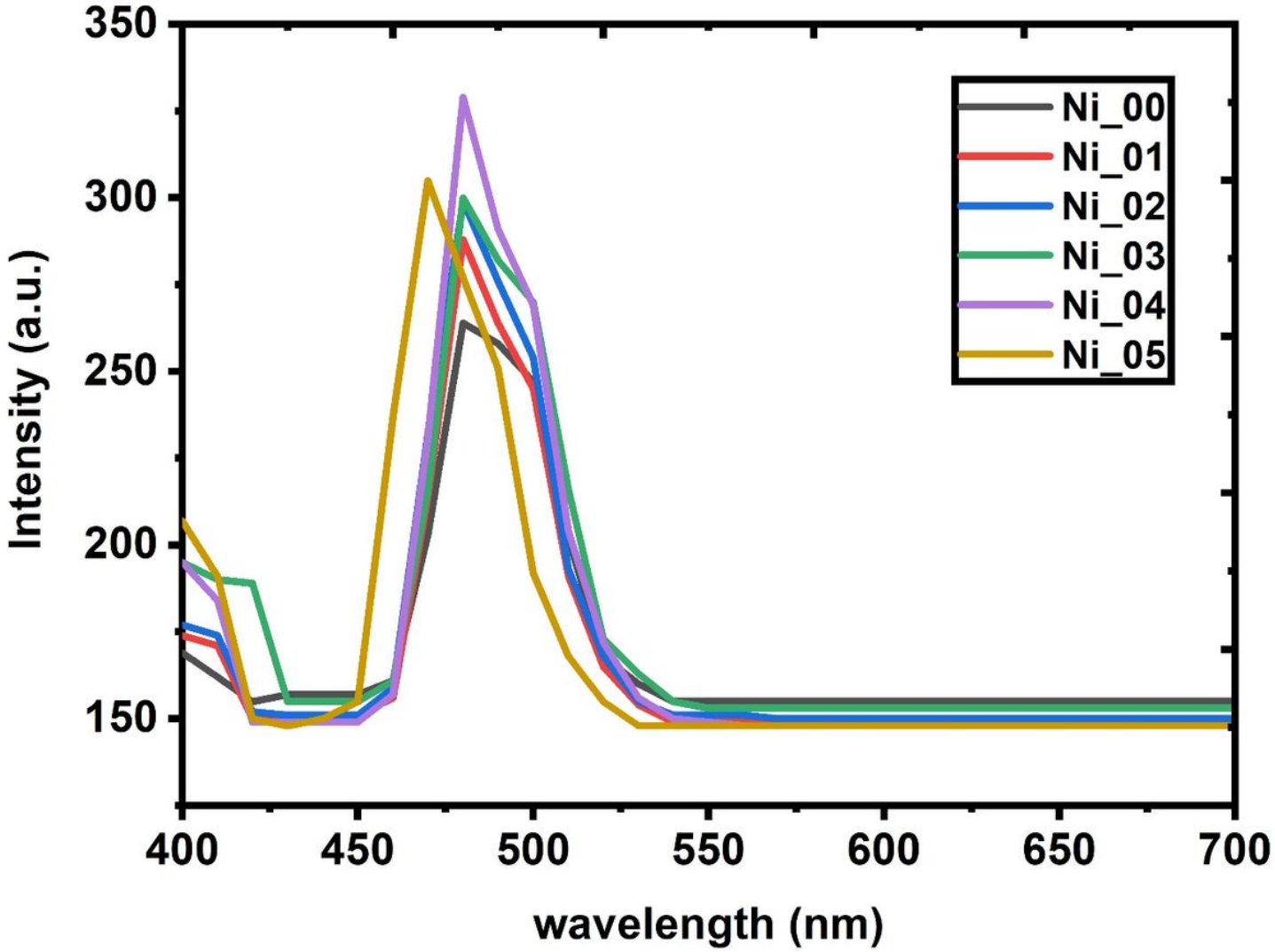

Figure 5

Photoluminescence spectra of nanocrystalline CdS thin films of undoped and Ni doped nanocrystalline CdS thin films.

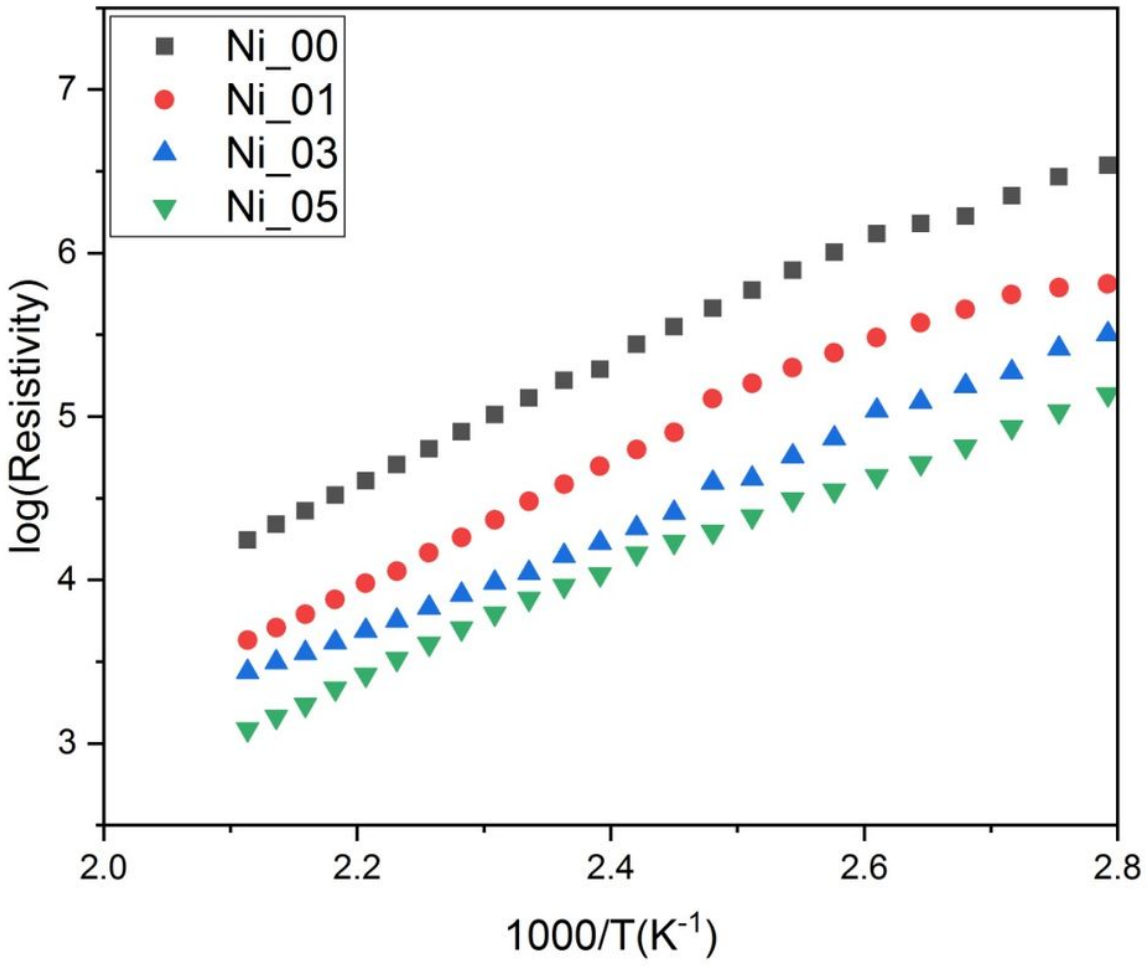

Figure 6

The plot of resistivity versus Temperature of nanocrystalline CdS thin films of undoped and Ni doped nanocrystalline CdS thin films

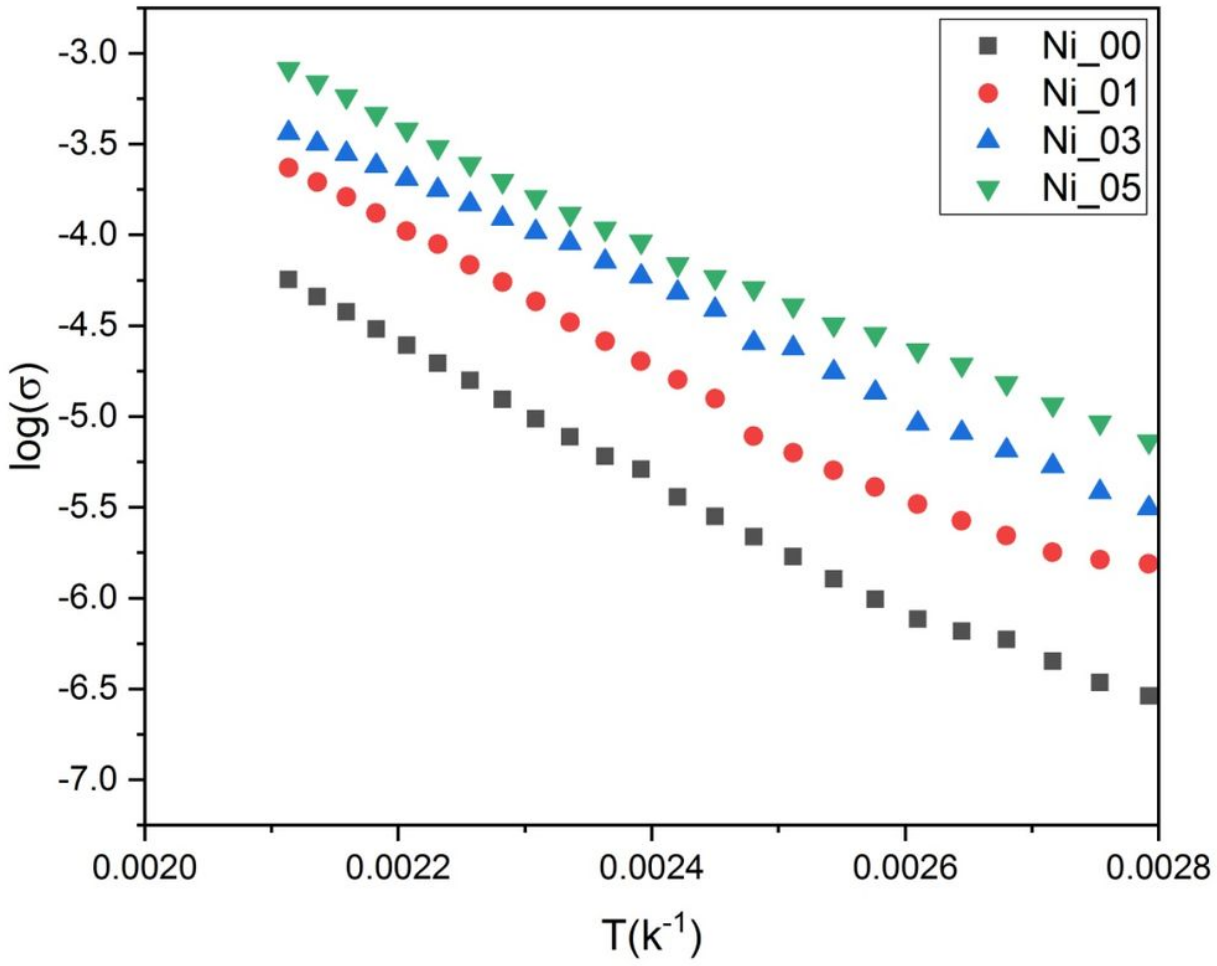

Figure 7

The plot of conductivity versus Temperature of nanocrystalline CdS thin films of undoped and Ni doped nanocrystalline CdS thin films